THE JOURNAL OF PHYSICAL CHEMISTRY C

Article

pubs.acs.org/JPCC

Structure and Dynamics of an Electrolyte Confined in Charged Nanopores

Pierre-Andre Cazade,[†,‡] Remco Hartkamp,[†,§] and Benoit Coasne*[,†,§,∥]

[†]Institut Charles Gerhardt Montpellier, UMR 5253 CNRS, Universite Montpellier, ENSCM, 8 rue de l'Ecole Normale, 34096 Montpellier Cedex 05, France

[‡]Department of Chemistry, University of Basel, Klingelbergstrasse 80, 4056 Basel, Switzerland

[§]MultiScale Materials Science for Energy and Environment, CNRS-MIT (UMI 3466), Massachusetts Institute of Technology, 77 Massachusetts Avenue, Cambridge, Massachusetts 02319, United States

[∥]Department of Civil and Environmental Engineering, Massachusetts Institute of Technology, 77 Massachusetts Avenue, Cambridge, Massachusetts 02319, United States

Supporting Information

ABSTRACT: Molecular Dynamics simulations are used to investigate the structure and dynamics of an aqueous electrolyte (NaCl) confined within a nanomembrane, which consists of a nanopore with a diameter 3 nm having a negatively charged surface. Both nanomembranes with a *diffuse charge* and with *local charges* are considered (in both cases, two surface charge densities are considered, −0.9 e/nm^2 and −1.8 e/nm^2). For all nanomembranes, significant layering of water and ions in the vicinity of the nanomembrane surface is observed. While the distribution of water and chloride ions is nearly insensitive to the nanomembrane charge and type, the arrangement of sodium cations within the nanomembrane depends on the system being considered. The water and ion density profiles in the nanomembranes are compared with the predictions of a modified Poisson−Boltzmann equation in which charge image, solvation effects, and dispersion interactions with the surface are taken into account [Huang et al. *Langmuir*, **2008**, *24*, 1442]. The self-diffusion coefficient for a given species is smaller than its bulk counterpart and is at most 75% of the bulk value. While the self-diffusion coefficients for water and sodium cations decrease with decreasing the overall negative charge of the nanomembrane, the self-diffusion coefficient for the chloride anions is nearly independent of the nanomembrane type and charge. We also estimate the dynamics of the confined aqueous electrolyte by calculating time correlation functions which allow estimating solvation, ion pairing, and residence times.

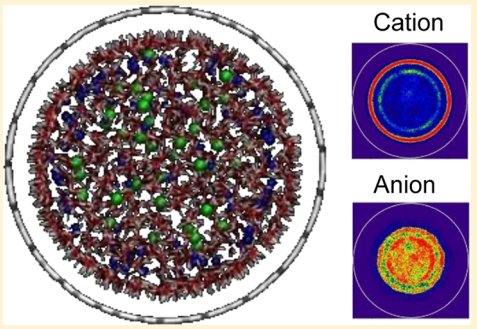

1. INTRODUCTION

Adsorption and transport of aqueous electrolytes in charged nanopores are relevant to many applications in the field of nanofluidics, treatment of wastewater and nuclear effluents, colloid stability and concrete aging, chromatography, etc.[1,2] Of particular importance in the field of water science, nanofiltration membranes are promising candidates for the treatment of wastewater and the production of drinkable water from seawater.[3,4] These membranes, which contain slightly charged pores at the nanometer scale, allow large volumes of water to be desalinated while selectively filtering ions.[5,6] They constitute a possible alternative to reverse-osmosis membranes which are energetically costly and require rejecting highly concentrated salt solutions into the sea.[7] Molecular simulation studies on confinement and transport of aqueous electrolytes in hydrophobic nanopores, i.e., a simplified model of nanofiltration membranes, were briefly reviewed in ref 8. By considering the series of sodium halides (NaX with X = F, Cl, Br, and I), we also addressed in ref 8 the physical origin of ion-specific effects on transport in nanochannels using polarizable force fields. As far as structural properties are concerned, the behavior of the NaF electrolyte solution was found to significantly differ from that of the other sodium halide solutions. Due to their small size, Na and F were found to be significantly solvated by water. In addition, due to steric and hydrophobic effects,[9] Cl, Br, and I tend to be repelled from the regions where the density of water is large. In contrast, ion-specific effects on the dynamics of water and ions were found to be minimized when the electrolyte solution is confined at the nanoscale in comparison to bulk water and the water−air interface.[10]

Real nanofiltration membranes possess a charged surface, which needs to be taken into account in order to clarify the physics and chemistry at play in nanofiltation processes. In particular, the electrical field created by the charged surface affects not only the structure of the electrolyte but also its transport due to diffusion, osmosis, and reverse osmosis. As a

Received: October 4, 2013
Revised: February 13, 2014
Published: February 17, 2014

   dx.doi.org/10.1021/jp4098638 | *J. Phys. Chem. C* 2014, 118, 5061−5072

result, many authors attempted to improve the classical model of the electrical double layer by including new contributions that account for confinement, surface-driven effects,[11−13] and size-dependent hydrophobic solvation energy of the ions.[14] However, discrepancies are observed between the theoretical models and molecular dynamics simulations when the pore size decreases below 1.5 nm or the surface charge increases beyond 1 e/nm^2.[15] From a molecular simulation point of view, the effect of the charged surface of the nanomembrane on the structure and dynamics of confined electrolytes has received little attention. Suk and Aluru[16] addressed the effect of an electric field on reverse osmosis in boronitride nanotubes. These authors reported that reverse osmosis is enhanced when an electric field is applied in the direction of the reverse-osmotic flow. This result is due to the orientation of the water dipole along the electric field, which facilitates their mobility and transport.

In this paper, we investigate by means of molecular simulations the effect of the charged surface on the structure and dynamics of an aqueous electrolyte confined in a charged nanomembrane. We also compare our molecular simulation results with the predictions of a modified Poisson−Boltzmann equation, which incorporates different interaction energies such as an ion-size-dependent hydrophobic solvation energy, the repulsive/dispersive energy between the ions and the charged surface, and a charge image contribution.[17] The modified Poisson−Boltzmann equation, which is solved for the cylindrical geometry corresponding to our system, also includes the effect of the polarization of the confined solvent calculated from the atomic density profiles of confined water.

In this work, we select a NaCl electrolyte of a concentration C = 1.85 mol/L. Polarizable force fields for both the water molecules and the ions are used as several molecular simulation studies on interfacial electrolytes (gas/liquid, liquid/liquid, and solid/liquid interfaces) have suggested the crucial role played by polarizability.[18−30] The nanomembrane is modeled as a single-walled carbon nanotube with a diameter 3 nm, which corresponds to an ideal system allowing researchers to clarify the physics involved in nanofiltration.[31] In addition to being a useful model for theoretical approaches of transport and confinement at the nanometric scale, carbon nanotubes are relevant to practical applications in nanofiltration and nanofluidics.[1,32] Both nanomembranes with a *diffuse charge* and with *local charges* are considered to determine the effect of the charge distribution on the structure and dynamics of the confined electrolyte (two surface charge densities are considered: −0.9 e/nm^2 and −1.8 e/nm^2). The structure and dynamics of the confined electrolyte are investigated by means of Molecular Dynamics (MD). This molecular simulation technique, which gives access to structural, dynamical, and thermodynamical properties, is well-suited to investigate the behavior of confined systems. In addition, periodic boundary conditions were used in order to mimic an infinite nanotube in the z direction. This approach, which contrasts with what is usually done (a long nanopore pore opened toward bulk reservoirs at its openings), is complementary to this general method.[33] Indeed, ion transport in nanofilters can approximately be broken down into three steps: partitioning into the nanopore from the external feed solution, transporting through the nanopore, and finally partitioning out of the nanopore into the external permeate solution. The approach adopted here allows us to focus in detail on the intermediate step of transport through the nanopore where diffusion and/or pairing-correlation effects modified by confinement with respect to the bulk may play an important role.

2. COMPUTATIONAL DETAILS

2.1. Models for the Electrolyte Solution and Charged Nanomembranes. A charged single-wall carbon nanotube is used as a model system of the channels in a nanofiltration membrane. A neutral carbon nanotube is first obtained by wrapping a graphene sheet around the x axis in the armchair conformation. The nanotube length is equal to 7.1 nm while its diameter is 3 nm. We consider two surface charge densities: −0.9 e/nm^2 and −1.8 e/nm^2. For each surface charge density, two types of nanomembranes are considered in order to address the effect of the nature of the electrostatic field on the structure and dynamics of the confined electrolyte: (1) a weak charge δq is attributed to each carbon atom of the nanomembrane (δq = −0.023 51 and −0.047 02 for the nanomembranes with surface charges of −0.9 e/nm^2 and −1.8 e/nm^2, respectively), and (2) a formal charge q = −1e is attributed to n carbon atoms selected periodically along the z axis (n = 60 and 120 for the nanomembranes with surface charges of −0.9 e/nm^2 and for −1.8 e/nm^2, respectively). In what follows, the first and second systems, which are illustrated in Figure 1, will be referred to as nanomembrane with a *diffuse charge* and nanomembrane with *local charges*, respectively. The confined aqueous NaCl electrolyte is modeled using polarizable force fields as it has been suggested that polarization is crucial for an accurate description of ionic solutions. Water is described in our simulations using the POL3 polarizable model of Caldwell and Kollman[34] In this model, each O and H atom of the rigid water molecule possesses a partial charge that interacts through Coulombic forces. In addition, the oxygen atom of the water molecule is a center of repulsion/dispersion interactions which interacts through a Lennard-Jones potential. The polarization contribution is included by taking into account the polarizabilities of both the oxygen and hydrogen atoms. Sodium cations and chloride anions of the aqueous electrolyte are described as single spheres with a formal charge (+1 for the cations and −1 for the anions). Each ion is a center of repulsion/dispersion interactions modeled using Lennard-Jones potentials. The Lennard-Jones parameters for the ions were taken from the work by Dang et al.[35−38] on bulk electrolyte solutions. Polarizabilities for the anions and cations were taken from refs 36−38.

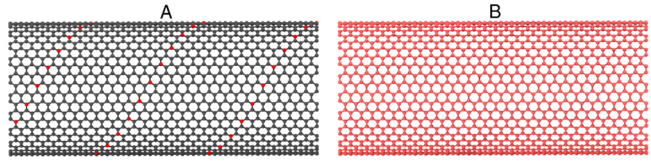

Figure 1. Molecular configurations showing the two types of charged nanomembranes modeled as a single-walled carbon nanotube with a diameter 3 nm. On the left-hand side (A), local charges are represented by red spheres and neutral carbons by gray spheres. On the right-hand side (B), all the carbon atoms bear a small charge and are shown as pink spheres.

Interactions between the ions, atoms of the water molecule, and carbon atoms of the nanomembrane were calculated as the sum of the Coulombic, polarization, and dispersion interactions with a repulsive short-range contribution. The energy of the atom or ion k at a position r_k is given by

dx.doi.org/10.1021/jp4098638 | J. Phys. Chem. C 2014, 118, 5061−5072

$$U_k(r_k) = \sum_j \left\{ 4\varepsilon_{jk}\left[\left(\frac{\sigma_{jk}}{r_{jk}}\right)^{12} - \left(\frac{\sigma_{jk}}{r_{jk}}\right)^{6}\right] + \frac{q_j q_k}{4\pi\varepsilon_0 r_{jk}} \right\} - \frac{1}{2}\boldsymbol{\mu}_k \cdot \mathbf{E}_k^{(0)} \quad (1)$$

where r_{jk} is the distance between atoms j and k (j, k = O, H, Na, Cl, or C). The first term in eq 1 is the repulsive term that corresponds to the repulsive energy due to finite compressibility of electron clouds when approaching the atom or ion to a very short distance from the nanomembrane surface or another atom or ion. The second term in eq 1 is the dispersion interaction. The energetic and geometric cross-parameters ε_{jk} and σ_{jk} were obtained from the like-atom parameters using the Lorentz–Berthelot mixing rules.[39] We note that ε_{jk} in eq 1 has to be expressed in Joules to be consistent with the Coulombic term. The third term in eq 1 is the Coulombic interaction between the charge of atom or ion k and that of atom or ion j. The fourth term is the polarization contribution of atom or ion k. $\boldsymbol{\mu}_k$ is the polarization dipole of the atom or ion k resulting from the interaction with the charges and dipoles j, and $\mathbf{E}_k^{(0)}$ is the electrostatic field at $\mathbf{r}_k$ due to all of the charges and dipoles j. The atomic parameters for the electrolyte/electrolyte and electrolyte/nanomembrane interactions are summarized in Table 1 (see also ref 8). Interatomic energy contributions were calculated within a cutoff radius equal to 1.2 nm. The Coulombic energy was computed using the Ewald summation technique with the following parameters: a Gaussian width equal to α = 2.27 nm^{-1} and k_{max} = 12, 12, 16 along the x, y, and z directions, respectively. The polarization energy was computed in the frame of the Car–Parrinello scheme,[40] which consists of affecting a fictitious mass to the induced dipole and integrating its trajectory at each time step of the molecular simulation run.

Table 1. Interaction Parameters of the Models Used for the Simulations[a]

atomic label	q_i (e)	α_i (10^{-3} nm^3)	ε_{ii} (kcal mol^{-1})	σ_{ij} (nm)
Na	1.000	0.240	0.100 00	0.233 59
Cl	−1.000	3.250	0.100 00	0.433 87
O (POL3)	0.730	0.528	0.156 00	0.320 37
H (POL3)	0.365	0.170		
C	0.000	0.000	0.055 64	0.340 00

[a] q_i is the partial charge, α_i the polarizability, ε_{ii} and σ_{ii} parameters for the Lennard-Jones potential.

2.2. Molecular Dynamics. The structure and dynamics of the aqueous electrolyte confined in the charged nanomembranes were simulated using classical Molecular Dynamics. Periodic boundary conditions in the three dimensions of space were used in order to mimic nanomembranes with infinite pores in the z direction. The size of the simulation box in the x and y directions was chosen large enough to ensure negligible interactions between the electrolyte solution confined in the carbon nanotube and its periodic images ($L_{x,y}$ = 7 nm). The temperature was set to 300 K, and the number of anion/cation pairs (42 pairs) was chosen to obtain a concentration of about 1.85 mol/L. Such a concentration, though rather high compared to regular seawater (0.6 mol/L), is a compromise between a sufficiently large number of ions to obtain reliable statistics, a reasonable number of water molecules due to the computational cost of polarization energy, and a value remaining in the range of known concentrations into seawater, 0.09–5.8 mol/L. A physically reasonable density of water molecules confined in the nanotube at a fugacity of 1 atm was obtained by first performing Grand Canonical Monte Carlo (GCMC) simulations (details can be found in refs 41–43). The net charges −0.9 e/nm^2 and −1.8 e/nm^2 of the nanomembranes were compensated by adding 60 and 120 Na cations in the electrolyte, respectively. The Molecular Dynamics simulations were performed with the AMBER 9 software.[44] The initial configurations were taken from the well-equilibrated GCMC calculations mentioned above. Trajectories were limited to 2 ns in order to keep the computing time reasonable. Trajectories were integrated in the frame of the leapfrog algorithm with a time step of 1 fs. The temperature was maintained constant using a Berendsen thermostat with a coupling time to the thermal bath equal to 0.1 ps. The properties and configurations of the system were stored every 1 ps.

3. RESULTS

3.1. Structure of Confined Electrolyte Solutions. *3.1.1. Molecular Simulation.* Figure 2 shows the density contour plots of the aqueous electrolyte confined in the nanomembranes with the *diffuse charge* and *local charges*, respectively. These contour plots represent a map of the radial density for the water molecules, chloride anions, and sodium cations within the nanomembrane (each density map is integrated over the whole nanotube length). Figure 2 also shows typical molecular configurations to illustrate the positions of the different species in the charged nanomembranes. For all nanomembranes, the contour plots for water exhibit density maxima located at well-defined positions from the nanomembrane surface. The amplitude of these maxima decreases with increasing the distance from the nanomembrane surface. These density oscillations reveal the significant layering of water in the vicinity of the nanomembrane surface. Such a spatial ordering of confined water is characteristic of water in hydrophobic or hydrophilic spaces.[45−54] The density of confined water tends toward the bulk value close to the pore center as the water molecules recover their bulk properties [this can be seen in the radial density profiles $\rho(r)$ provided in the Supporting Information (Figure S1)]. The density contour plots for confined water are nearly insensitive to the type (*local charges* versus *diffuse charge*) and charge of the nanomembrane (−0.9 e/nm^2 versus −1.8 e/nm^2). In addition, the ordering of water confined in the charged nanomembrane is very similar to what was obtained for neutral nanochannels.[8] This result shows that, even for salt concentrations 3 times larger than that of seawater (~0.6 mol/L), the structure of water confined in charged nanomembranes is mainly driven by the dispersion–repulsion interactions between water and the nanomembrane.

The density contour plots for sodium cations in the nanomembranes with a *diffuse charge* also exhibit density oscillations. Again, this result shows that the sodium cations tend to form layers at the nanomembrane surface (Figure 2a). In contrast to what was observed for water, such a spatial ordering of confined cations is sensitive to the charge of the nanomembrane as it depends on a subtle competition between the water/cation and cation/charged surface interactions. On the one hand, for the highly charged nanomembrane (−1.8 e/nm^2) with a *diffuse charge*, cations form a layer at a position r =

dx.doi.org/10.1021/jp4098638 | J. Phys. Chem. C 2014, 118, 5061−5072

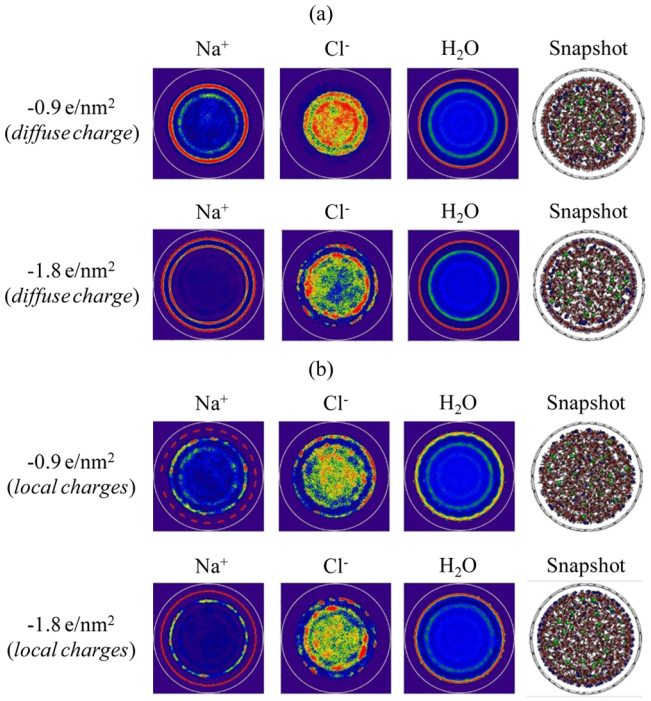

Figure 2. (a) Contour plots showing the density distribution of sodium ions Na, chloride ions Cl, and water for an aqueous electrolyte NaCl (1.85 mol/L) at location (*x*,*y*) in a charged nanomembrane carrying a diffuse charge: −0.9 e/nm^2 (top) and −1.8 e/nm^2 (bottom). The density increases from blue, green, yellow, orange, and red. (b) Contour plots showing the density distribution of sodium ions Na, chloride ions Cl, and water for an aqueous electrolyte NaCl (1.85 mol/L) at location (*x*,*y*) in a charged nanomembrane carrying local charges: −0.9 e/nm^2 (top) and −1.8 e/nm^2 (bottom). The density increases from blue, green, yellow, orange, and red. For each contour plot, the associated radial density profiles are provided as Supporting Information. r = 0 and 1.5 nm correspond to the center of the nanomembrane and the wall of the nanomembrane, respectively. A typical molecular configuration is also shown for each system. Gray segments are bonds between the carbon atoms of the nanomembrane while the white and red segments are the water molecules. Blue and green spheres are the Na and Cl ions, respectively.

1.28 nm in contact with the nanomembrane due to the strong interaction with its charged surface. Beyond this first adsorbed layer, cations tend to occupy the porous space in a more homogeneous manner although some layering is still observed. This result shows that cation ordering in the highly charged nanomembrane is mainly driven by the interaction between the cations and the charged surface. On the other hand, for the weakly charged nanomembrane (−0.9 e/nm^2) with a *diffuse charge*, the surface charge is not strong enough to induce the formation of an adsorbed layer of cations in contact with the nanomembrane surface; in contrast, the sodium cations tend to be distributed in between the first two adsorbed layers of water molecules where the water density is low. This result suggests that the positional ordering of the cations for the weakly charged nanomembrane with a *diffuse charge* is governed by their interaction with the confined water molecules and not by their interaction with the charged nanomembrane surface. This result is confirmed by the fact that the positions of the cation layers for this weakly charged nanomembrane are very similar to those obtained with the same nanomembrane carrying no charge.[8] This configuration where sodium cations are sandwiched between water layers is favorable as it leads to enhanced solvation of the cations while being compatible with the layering imposed by the nanomembrance surface. Such a significant solvation of sodium cations is due to their small size, which only weakly disturbs the hydrogen bonding between water molecules. In addition, the cations tend to be repelled from the surface because of steric and dielectric effects, which arise from the dielectric discontinuity between water in the nanomembrane and water-depleted region near the nanomembrane surface. In contrast to the results above, the density contour plots for sodium cations in the nanomembranes with *local charges* exhibit density oscillations, which are nearly insensitive to the charge of the nanomembrane (Figure 2b). The positions and amplitudes of the density peaks for the nanomembranes with *local charges* are similar to those observed for the nanomembrane with a *diffuse charge* having the highest charge (−1.8 e/nm^2).

For all charged nanomembranes, the density contour plots for chloride anions also exhibit density oscillations as chloride tends to be adsorbed in concentric layers. These layers are located close to the pore center with respect to the outermost layer of sodium cations as chloride anions carry a negative charge of the same sign as the nanomembrane so that they cannot be adsorbed in contact with the surface. The ordering observed for the chloride anions is less marked than for the sodium cations as the former occupy the porous space in a more homogeneous way. This departs from what we observed in our previous work for uncharged nanomembranes in which chloride was found to form well-defined adsorbed layers. This result shows that the pronounced layering of the sodium cations, which is induced by their interaction with the charged nanomembrane surface, affects the solvation properties of the confined chloride anions.

3.1.2. Modified Poisson−Boltzmann Equation. Various theoretical and empirical methods exist that attempt to describe the electric double layer (EDL) of confined electrolyte solutions or ionic liquids. These methods are often based either on the Poisson−Boltzmann (PB) equation or on Density Functional Theory (DFT). Both methods are well-established and have proven very useful under certain conditions. However, there is a large interest in extending these methods to describe the EDL in a system under different conditions, or simply for a broader range of conditions. Of special interest are situations where the surface charge density or the ion concentration is large; such cases can lead to phenomena such as overscreening, crowding, and strong variations in the local permittivity.[55] As pointed out in ref 56, the approach of using any continuum model to predict phenomena that occur on a molecular scale has some limitations. Gillespie and co-workers have developed a DFT approach to describe the structure of ions confined in nanopores or adsorbed at surfaces.[57] Such an approach in which properties of the confined solution are treated as nonhomogeneous quantities is able to capture any set of experimental or simulation data provided enough terms are included to describe the physics at play (solvent layering, different types of interaction, etc.). In the present work, instead of using such an approach, we attempt to describe our molecular simulation results using a much simpler approach: a modified but still simple PB equation. The PB model is a classical theory that describes the electrical double layer formed by an electrolyte solution in contact with a solid surface or confined in pores. This theory combines the Poisson equation, which relates the electrostatic potential to the charge density, and the Boltzmann equation that describes the density

dx.doi.org/10.1021/jp4098638 | J. Phys. Chem. C 2014, 118, 5061−5072

distribution of the ionic species in thermodynamic equilibrium. The PB equation rests on a number of assumptions. For instance, only Coulombic interactions are included in the equation, the finite size of the ions is not taken into account, the aqueous solution is assumed to be a continuous medium with a dielectric constant that does not depend on the position, and ion−ion correlations and fluctuations are not taken into account since it is a mean-field theory. Mixed successes have been achieved by adding correction terms to the classical PB equation to overcome some of these shortcomings. Following the work by Bocquet and co-workers,[17,58] we apply two models to predict the charge density profile of the electrolyte solution in water. The first model, presented by Joly et al.,[54] is based on the assumption that the ionic charge distribution is modulated by the free energy profile of the solvent, $k_BT\ln(\rho_f(r)/\rho_{f,bulk})$

$$\rho_{\pm}(r) = \rho_0 \exp(\mp\beta e V(r))\frac{\rho_f(r)}{\rho_{f,bulk}} \tag{2}$$

where ρ_0 is the bulk ion density, $V(r)$ is the electrostatic potential, $\rho_f(r)$ is the solvent density profile, and $\rho_{f,bulk}$ is the solvent density in the center of the tube. The second model considered here includes a correction term to account for non-Coulombic interactions between the aqueous electrolyte and its surrounding. This correction appears in the form of an external potential $U^{ext}_{\pm}(r)$ added to the exponent in the Boltzmann equation so that the ion charge density for a species in thermodynamic equilibrium is given by

$$\rho_{\pm}(r) = \rho_0 \exp(-\beta(\pm eV(r) + U^{ext}_{\pm}(r))) \tag{3}$$

where the external potential $U^{ext}_{\pm}(r) = U^{im}(r) + U^{LJ}_{\pm}(r) + U^{hyd}_{\pm}(r)$ is given by the sum of an image potential, an effective ion-wall Lennard-Jones contribution, and the hydrophobic solvation energy. The first and last contributions in $U^{ext}_{\pm}(r)$ are taken from ref 17, whereas the Lennard-Jones contribution is calculated specifically for our system. These terms are described in more detail in the Supporting Information. Besides the influence of non-Coulombic interactions, following ref 17, we also add a term to the Poisson equation to account for position-dependent polarization $P(r)$ of the medium.

The Poisson equation for a cylindrical geometry is given by

$$\frac{1}{r}\frac{d}{dr}\left(-\varepsilon_0 r\frac{dV(r)}{dr}\right) + \frac{dP(r)}{dr} = \rho_e(r) \tag{4}$$

where ε_0 is the vacuum permittivity constant, $\rho_e(r) = e[\rho_+(r) - \rho_-(r)]$ is the ionic charge density, and $P(r)$ represents the position-dependent polarization of water in the system. Following ref 17, two assumptions are considered to quantify $P(r)$: (1) a simple step polarization (SP) equation in terms of the gradient of the potential field and (2) a full polarization (FP) model that uses charge density profile calculated from the molecular simulation. While the FP approach should, in principle, lead to very accurate predictions, it requires estimating from atomistic simulations (such as in the present work) the density profile of vicinal or confined water. As a result, this approach is limited as it does not allow predicting the behavior of confined electrolytes without having to perform time-consuming molecular simulations. In contrast, the SP polarization is a simpler approach which does not require performing molecular simulations but still captures the physics at play. Combining eqs 3 and 4 results in a modified Poisson−Boltzmann (MPB) equation. We solve this equation numerically using an iterative method to relax to the electric potential profile from an initial guess to a solution of the differential equation. Neumann boundary conditions are applied at the charged surface $\left.\frac{dV}{dr}\right|_{r=r_{wall}} = -\frac{\sigma_s}{\varepsilon_0\varepsilon_w}$, where $\varepsilon_w = 78$ is the permittivity constant for bulk water, and in the center of the channel, $\left.\frac{dV}{dr}\right|_{r=0} = 0$, where a zero slope of the potential is required because of the symmetry of the system. The total charge density profile can then be calculated by substituting the electrostatic and external potential into eq 2. More details on the MPB equation and how to solve it can be found in the Supporting Information.

Figure 3 shows the charge density profiles for the systems with the localized charges and the system with diffuse charges.

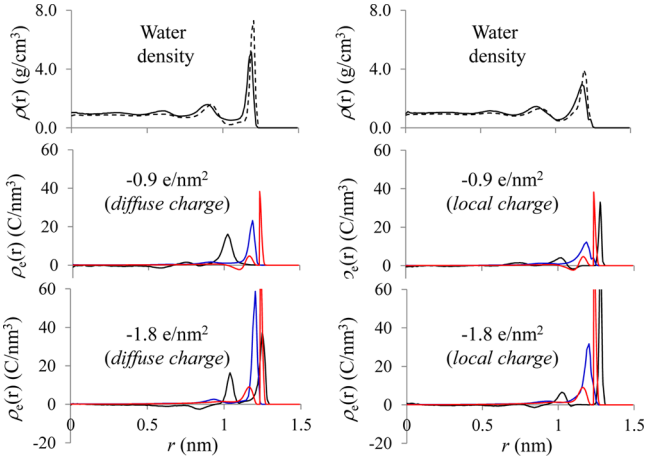

Figure 3. (Top) Water density profile for a carbon nanotube with a diffuse surface charge (left) and a local surface charge (right). The profiles are shown as a function of the radial position in the channel, with $r = 0$ corresponding to the center of the tube and $r = 1.5$ nm the wall position. The solid and dashed lines are for the surface charge equal to −0.9 e/nm² and −1.8 e/nm², respectively. (Middle) Ionic charge density of aqueous electrolyte NaCl (1.85 mol/L) in a carbon nanotube with a diffuse charge (left) and a local charge (right). The black lines are the molecular simulation data while the solutions to the two variants of the modified Poisson−Boltzmann equation are indicated with different colors, blue for the model of Joly et al. and red for the step polarization (SP) model. The total surface charge is equal to −0.9 e/nm². (Bottom) Same as top but for a total surface charge is equal to −1.8 e/nm².

We show both the results of the MD simulations and the different solutions of the modified Poisson−Boltzmann equations: the approach by Joly et al. and the solution with the SP approach (we note that, for the sake of clarity, we do not show the data obtained using the FP approach as they were found very close to those corresponding to the SP approach). Figure 3 also shows the density profile of the oxygen atoms in the solvent for comparison. Figure 3, left, corresponds to a diffuse surface charge density of −0.9 e/nm² and −1.8 e/nm², respectively. Figure 3, right, shows results for the cases where the surface charges are localized. As expected, the average density of the anions is lower than that of the cations in order to counterbalance the negative surface charge of the system. On the other hand, their bulk density, i.e., at positions far from the surface, is equal when the electrostatic potential created by the charged wall atoms becomes negligible. Hence, a larger density of cations is expected close to the wall, which results in a

dx.doi.org/10.1021/jp4098638 | J. Phys. Chem. C 2014, 118, 5061−5072

positive peak in the charge density profile near the wall (on the right, r = 1.5 nm) and a surface under the charge density profile that balances the negative wall charge (taking into account integrating over polar coordinates). These expectations are confirmed by the Molecular Dynamics results in Figure 2, which shows that a layer of cations is located between the solvent and the wall (with the exception of the system with a diffuse surface charge density of −0.9 e/nm^2 as discussed earlier). This result shows that the assumption used in the model by Joly et al., i.e., that the ion density is modulated by the free energy of the solvent (eq 2), does not capture the subtle interplay between solvent layering and ion solvation in between the solvent layers. In other words, the position of water density maxima does not necessarily coincide with favorable locations for ion adsorption since other positions such as in between the water density maxima leads to high ion solvation without strong steric repulsion. The numerical solutions of the modified Poisson−Boltzmann equation with the SP and FP models are very close to each other for each of the systems. This result confirms that the SP approach, which is less cumbersome as it does not require estimating the water density profile from atomistic molecular simulations, captures the physics at play. The location of the peaks is the same for either approach, which indicates that the location of the peaks is determined predominantly by the external potential, rather than by the inclusion of the polarization term. Even completely removing the polarization term only has a small effect on the solution of the MPB equation (result not shown). Thus, we find that using Molecular Dynamics data to predict the ionic charge density profile does not lead to an improved result, either through Joly's approach or by applying the FP model. The location of the first peak near the wall is largely dependent on the location of the minimum in the external potential. For this reason, removal of any of the three contributing terms in the external potential leads to a shift of the peak in the predicted charge density profile. Similarly, optimizing these terms could improve the predictive quality of the MPB model, at least for the prediction of the first positive peak. Note that the physical interpretation of the position and the magnitude of the peak (and similarly the position and well-depth of the energy potential) are closely related to the size of the ions. The fact that the size of the ions is not explicitly taken into account in our model could result in an overestimation of the ion concentration near a strongly charged surface; the maximum density of point charges is not constrained by a closed packing the way that finite-sized ions are. Despite the ability to predict the peak nearest to the wall, none of the models proves successful in predicting the rest of the charge density profile. We believe that this result is due to the fact that the ion density and surface charge are larger than the values where Poisson−Boltzmann is expected to give a reasonable prediction. Additional correction terms could be applied to the Poisson−Boltzmann equation in an attempt to improve the agreement between the theory and simulation result further. The aforementioned shortcomings of the traditional Poisson−Boltzmann equation can be addressed directly by adding terms that account for steric effects (i.e., finite size of ions) and ion−ion correlations. A vast number of theoretically or empirically derived correction terms have been presented in the literature.[59−68] The pioneering work of Bikerman[69] presented a very simple MPB equation that contained particle-size dependence. His model basically adds an excess term to the free energy function that accounts for the finite volume fraction taken up by the ions. This energy contribution equals the ideal entropy of mixing, as has later been shown. The resulting MPB equation is still used due to its simplicity and elegance. The model is shown and applied in the Supporting Information to see to what extent an inclusion of the ion size in the model affects the results for our system. While we find that the correction term has a small yet visible effect on the maximum ion concentration, the location of the peaks has remained unchanged.

Another known shortcoming of the PB theory is that it assumes that the surface charge is distributed homogeneously, whereas in reality the charges are carried by atoms and are thus localized. How this simplification of the PB theory affects its accuracy can be clearly seen by comparing results of our "diffuse" case (Figure 3, left) in which the total surface charge is equally distributed over all wall atoms and the "local" case (Figure 3, right) where only a small subset of the wall atoms is charged. In both cases the charge is assigned to atoms and thus not homogeneously distributed over the surface, but the level of smearing is very different. The SP and FP models successfully predict the location of the first peak near the wall for the diffuse case, whereas the local charges lead to a clear discrepancy between theory and simulation, as expected. As pointed out previously, the Molecular Dynamics simulation results of the system with a diffuse surface charge density of −0.9 e/nm^2 do not show a layer of cations between the solvent and the wall. Instead, the positions of the first layer of both ion species are approximately equal to the position of the second layer in the other three systems. This result could indicate that there is an energy barrier between the bulk and the wall region that is larger than the average thermal energy of the ions. Consequently, the event of crossing such a barrier would be associated with a small probability, such that the corresponding transition frequency is small relative to the typical time scale in molecular simulations. This would have to be investigated by calculating the free energy landscape, which is not part of this work.

The structure of the confined aqueous electrolyte was further determined by calculating pair correlation functions $g(r)$ between the different species. Such pair correlation functions are useful to estimate the structure of the confined solution as they are related to the probability of having an atom or ion at a given distance r from another atom or ion. They provide similar information to that gained from the structure factor $S(q)$ measured in X-ray diffraction experiments [$g(r)$ and $S(q)$ are related through Fourier transformation]. Figure 4 shows the pair correlation functions between the sodium cations and oxygen atoms of the water molecules and between the chloride anions and hydrogen atoms of water. We also show in Figure 5 the pair correlation function between the sodium cations and chloride anions of the confined electrolyte. For each pair correlation function, we report the results obtained for the four different charged nanomembranes (two surface charges with either *local charges* or a *diffuse charge*). The pair correlation functions in Figures 4 and 5 are characteristic of aqueous electrolytes. For all systems, the $g(r)$ function between the sodium cations and the oxygen atoms of water exhibits two pronounced peaks at r = 0.23 nm and r = 0.45 nm, which correspond to the first and second solvation shells of the sodium cation, respectively. Such marked correlations arise from the strong Coulombic interaction between the positive charge of the sodium cation and the negative charge of the oxygen atom of water. Similarly, the $g(r)$ function between the

dx.doi.org/10.1021/jp4098638 | J. Phys. Chem. C 2014, 118, 5061−5072

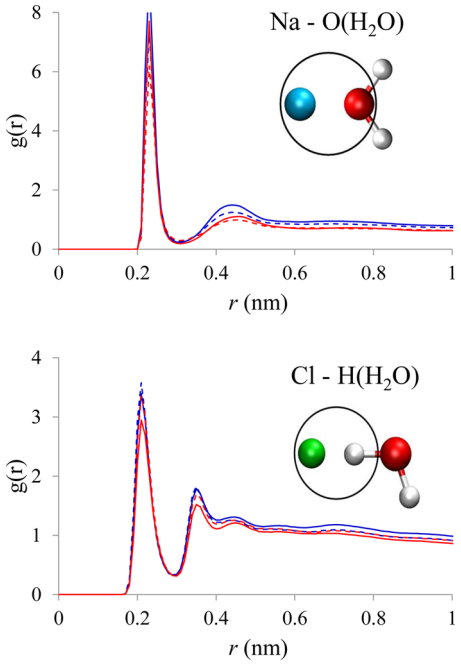

Figure 4. (a) Pair correlation function $g(r)$ between the sodium cations Na and the oxygen atoms O of the water molecules for an aqueous electrolyte NaCl (1.85 mol/L) confined in a charged nanomembrane with a diameter D = 3 nm carrying either a *diffuse charge* (solid lines) or *local charges* (dashed lines). The blue and red data are for a total electrostatic charge of −0.9 e/nm^2 or −1.8 e/nm^2. (b) Pair correlation function $g(r)$ between the chloride anions Cl and the hydrogen atoms H of the water molecules for an aqueous electrolyte NaCl (1.85 mol/L) confined in a charged nanomembrane with a diameter D = 3 nm carrying either a *diffuse charge* (solid lines) or *local charges* (dashed lines). The blue and red data are for a total electrostatic charge of −0.9 e/nm^2 or −1.8 e/nm^2.

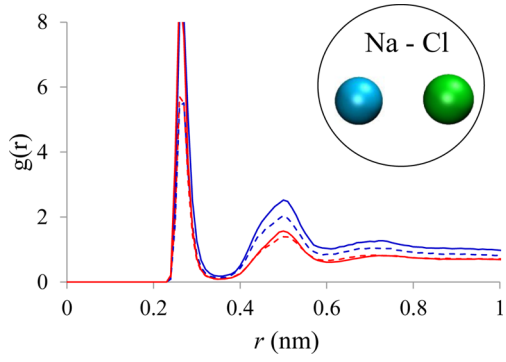

Figure 5. Pair correlation function $g(r)$ between the sodium cations Na and the chloride anions of an aqueous electrolyte NaCl (1.85 mol/L) confined in a charged nanomembrane with a diameter D = 3 nm carrying either a *diffuse charge* (solid lines) or *local charges* (dashed lines). The blue and red data are for a total electrostatic charge of −0.9 e/nm^2 or −1.8 e/nm^2.

chloride anions and the hydrogen atoms of water exhibits two pronounced peaks at r = 0.21 nm and r = 0.35 nm, which correspond to the first and second solvation shells of the anions. The $g(r)$ function in Figure 5 exhibits a marked peak at a distance r = 0.26 nm, which corresponds to the pairing between the sodium cations and chloride anions driven by the attractive Coulombic interaction. A second peak is observed at a distance $r \sim 0.5$ nm, which corresponds to sodium and chloride ions separated by a water molecule.

For a given surface charge, the pair correlations involving the sodium cation [Na−O(H_2O) and Na−Cl] show that the correlations are less marked (less intense peaks) for the nanomembrane with the *local charges* than with the *diffuse charge*. This result is due to the fact that the adsorption/layering of the sodium cations at the membrane surface is more important for the system with the *local charges* so that they interact less with the confined solvent (water) or chloride anions. The latter interpretation is confirmed by the fact that the amplitude of the peaks corresponding to the sodium−water correlations and to the sodium−chloride correlations decreases as the overall charge of the nanomembrane increases; i.e., as the total charge increases, the sodium cations get more strongly physisorbed at the membrane surface through the Coulombic interaction so that they interact less with the water molecules or chloride anions which tend to be located in the pore center. In contrast to the results above, the pair correlation function between the chloride anions and hydrogen atoms of water does not obey the same trends when the type and charge of the nanomembrane vary. This result is due to the fact that the structure of the confined chloride anions does not directly depend on the negative surface charge; for all systems, the interaction between the chloride anions and the negatively charged surface is screened as the sodium cations are located between the anions and the nanomembrane surface. In fact, the structure of the confined chloride anions rather depends on the exact position of the water molecules so that it cannot be directly related to the surface charge and type of charged nanomembrane.

3.2. Dynamics of Confined Electrolyte Solutions. The dynamics of confined electrolyte solutions is known to play a key role in nanofiltration processes which are based on weakly charged hydrophobic nanomembranes. In this work, we first investigated the dynamics of the confined electrolyte by calculating the mean square displacements (MSD) for all the species Na, Cl, H_2O. As will be discussed below, we checked that our simulation runs are long enough to reach the Fickian diffusive regime. Nevertheless, a drift of the center of mass (CoM) of the electrolytes was observed for both the nanomembrane with the *diffuse charge* and that with the *local charges*. Such a drift is due to the small number of water molecules and ions in the system (far from the thermodynamic limit), which implies that the initial distribution of velocities is not strictly Gaussian. As a result, given that only conservative forces are considered in our calculations, there is a nonzero displacement of the CoM that propagates in the entire course of the simulation. In order to correct our results for such a drift, the CoM displacement was subtracted in the analysis of the dynamical properties.[70] For an interesting discussion on the dynamics in small nanopores, see the papers by Hahn and Karger[71] and Moore et al.[72,73]

Figures 6 and 7 show the MSD along the nanomembrane axis z for the sodium cations, chloride anions, and water molecules of the electrolyte confined in the charged nanomembranes. Both the results for the nanomembranes with the *diffuse charge* and the *local charges* are reported. In agreement with previous studies on the dynamics of fluids confined in nanopores,[74−78] we found that the MSD in the direction perpendicular to the pore surface (results not shown) increases very rapidly at short times and then exhibits a plateau at larger times. This result shows that, due to radial confinement, there is

dx.doi.org/10.1021/jp4098638 | J. Phys. Chem. C 2014, 118, 5061−5072

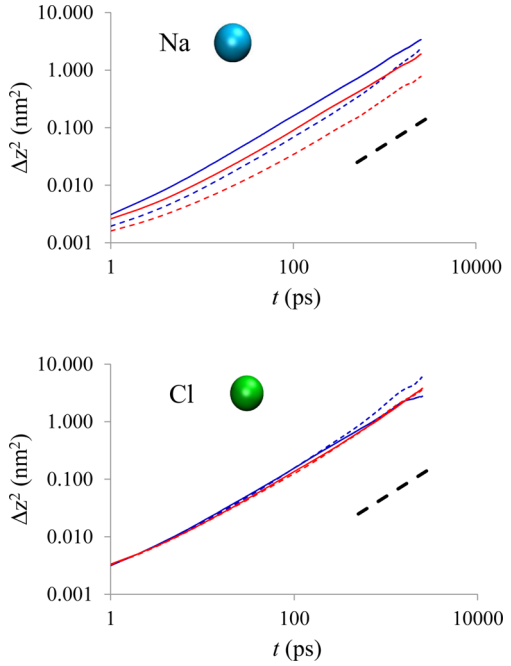

Figure 6. (a) Mean square displacements (MSD) along the nanomembrane axis for the sodium cations Na of an aqueous electrolyte NaCl (1.85 mol/L) confined in a charged nanomembrane with a diameter D = 3 nm carrying either a *diffuse charge* (solid lines) or *local charges* (dashed lines). The blue and red data are for a total electrostatic charge of −0.9 e/nm^2 or −1.8 e/nm^2. (b) Mean square displacements (MSD) along the nanomembrane axis for the chloride anions Cl of an aqueous electrolyte NaCl (1.85 mol/L) confined in a charged nanomembrane with a diameter D = 3 nm carrying either a *diffuse charge* (solid lines) or *local charges* (dashed lines). The blue and red data are for a total electrostatic charge of −0.9 e/nm^2 or −1.8 e/nm^2.

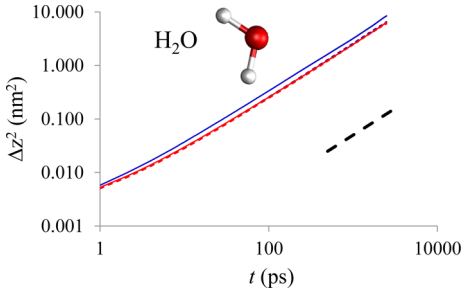

Figure 7. Mean square displacements (MSD) along the nanomembrane axis for the water molecules H_2O of an aqueous electrolyte NaCl (1.85 mol/L) confined in a charged nanomembrane with a diameter D = 3 nm carrying either a *diffuse charge* (solid lines) or *local charges* (dashed lines). The blue and red data are for a total electrostatic charge of −0.9 e/nm^2 or −1.8 e/nm^2.

no diffusion perpendicularly to the pore surface. For all species, the MSD along the nanopore axis z reaches the Fickian diffusive regime at long times where $\Delta z^2 \sim t$. In order to characterize the dynamics of the water molecules and ions confined in the charged nanomembranes, we calculated their self-diffusion coefficient D_z from the derivative of Δz^2 with respect to time:

$$D_z = \lim_{t\to\infty} \frac{1}{2}\frac{\mathrm{d}\langle (z(t) - z(0))^2\rangle}{\mathrm{d}t} \quad (5)$$

D_z values are shown in Table 2 for water, sodium cations, and chloride anions confined in the charged nanomembranes

Table 2. Self-Diffusion Coefficients D of Water Molecules and Ions for an Aqueous Electrolyte NaCl (1.85 mol/L) Confined in a Charged Nanomembrane with a Diameter 3 nm Carrying Either a Diffuse Charge or Local Charges[a]

species	neutral nanomembrane	charged membrane carrying a *diffuse charge*		charged membrane carrying *local charges*	
surface charge (e/nm^2)	0.0	−0.9	−1.8	−0.9	−1.8
D_{Na+} (10^{-5} cm^2/s)	0.65	0.70	0.40	0.44	0.16
D_{Cl-} (10^{-5} cm^2/s)	0.90	0.70	0.70	0.70	0.70
D_{H2O} (10^{-5} cm^2/s)	1.33	1.65	1.25	1.28	1.22

[a]The total surface charge of the nanomembrane is −0.9 e/nm^2 or −1.8 e/nm^2. We also report the data for the same electrolyte confined in a neutral nanomembrane. The bulk self-diffusion coefficients for the same electrolyte are $D_{Na+} = 0.98 \times 10^{-5}$ cm^2/s, $D_{Cl} = 1.50 \times 10^{-5}$ cm^2/s, $D_{H2O} = 2.20 \times 10^{-5}$ cm^2/s.

carrying a *diffuse charge* or *local charges*. We also report the values D_z^0 obtained for the same system but confined in a neutral nanomembrane.[8] For all nanomembranes (charged and uncharged), the self-diffusion coefficient for a given species is smaller than its bulk counterpart, $D_z < 0.75D_z^0$. Both the self-diffusion coefficients for water and sodium cations decrease with increasing the charge of the nanomembrane. This result is due to the fact that the strong interactions between the sodium cations or the water molecules and the charge of the nanomembrane tend to slow down their dynamics. In addition, for a given surface charge, the self-diffusion coefficients of the sodium cations and the water molecules are lower for the nanomembrane with *local charges* than for the membrane with a *diffuse charge*. This is due to the fact that the sodium cations tend to be more localized and, hence, less mobile as they are adsorbed in charged sites of the nanomembranes with *local charges*. In contrast to the results above, the self-diffusion coefficient for the chloride anions, $D_z \sim 0.7 - 0.8 \times 10^{-5}$ cm^2/s, is nearly insensitive to the charge of the nanomembrane. This can be explained by the fact that the anions tend not to interact with the negatively charged surface (in contrast to the cations and water molecules which strongly interact with the surface). Consequently, while the dynamics of the Na cations and water molecule is strongly affected by the membrane charge, the dynamics of the anions is nearly insensitive to the membrane charge. Finally, except for the charged nanomembrane with a *diffuse charge* of −0.9 e/nm^2, the self-diffusion coefficients of all the confined species are always smaller than those observed for the neutral nanomembrane. Such a slowing down of the confined electrolyte, which is induced by the surface charge of the nanomembrane, arises from the strong Coulombic interaction between the ions or the water molecules and the charged atoms of the nanomembrane. In contrast, the faster dynamics observed for the electrolyte confined in the weakly charged nanomembrane carrying a *diffuse charge* (with respect to that for the neutral nanomembrane) is due to the fact that, for this system, the surface charge is not strong enough to induce the formation of an adsorbed layer of cations in contact with the nanomembrane surface. As a result, we have seen above that the sodium cations tend to be adsorbed in between the first two layers of adsorbed water molecules where the

dx.doi.org/10.1021/jp4098638 | J. Phys. Chem. C 2014, 118, 5061−5072

water density is mimimum. Such a particular ordering of the confined electrolyte leads to faster diffusion of the water molecules as they are directly in contact with the nearly hydrophobic surface of the nanomembrane (in contrast, for the other systems, water is isolated from the carbon surface by the sodium cations which compensate the charge of the nanomembrane).

We further estimated the dynamics of the aqueous electrolyte confined in the charged nanomembranes by calculating the following time correlation function $R(t)$

$$R(t) = \frac{1}{N_i N_j} \sum_{i=1}^{N_i} \sum_{j=1}^{N_j} \langle \Theta_{ij}(0)\Theta_{ij}(t) \rangle \quad (6)$$

where $R(t)$ can be calculated between water molecules, anions, and cations. $\Theta_{ij}(t)$ equals 1 if i and j are nearest neighbors at time t and 0 otherwise. i and j are considered nearest neighbors if the distance r_{ij} is smaller than the first minimum in the corresponding $g(r)$ function shown in Figures 4 and 5. The brackets in eq 5 indicate that the value is averaged over a large number of Molecular Dynamics configurations. Because of the definition given above, $\Theta_{ij}(0)\Theta_{ij}(t) = 1$ if i and j are nearest neighbors at the times 0 and t. Consequently, $R(t)$ gives the probability of having i and j paired at times 0 and t. Such time correlation functions allow estimating the average solvation times of the cations by the water molecules.[8,41,79] In particular, these correlation functions can be related to NMR relaxometry data.[80,81] Figure 8 shows $R(t)$ between the sodium cations and the oxygen atoms of water and between the chloride anions and the hydrogen atoms of water, respectively. The results for the aqueous electrolyte confined in the different charged nanomembranes with *local charges* or a *diffuse charge* are reported. In contrast to the self-diffusion coefficients discussed above, the time correlation functions shown in Figure 8 cannot be interpreted in a straightforward manner (i.e., no obvious dependence on the charge or type of nanomembrane). Nevertheless, both sets of data, which follow the same trend and seem to be driven by a subtle balance between the average diffusivity and distribution of the confined aqueous electrolyte, can be rationalized as follows. The fastest decay in the time correlation functions (corresponding to the shortest Na−Cl pairing and Na solvation times) is observed for the weakly charged nanomembrane carrying a *diffuse charge*. Such short Na solvation times and Na−Cl pairing times are due to the fast diffusion of the confined species for this system (see Table 2); i.e., ions and water tend to stick to each other on shorter time scales as their molecular motions become faster. In contrast, the slowest decay in the time correlation functions is observed for the highly charged nanomembrane carrying a *diffuse charge*. In this case, given the strong Coulombic interaction between the numerous charges at the nanomembrane surface and the sodium cations, the latter are strongly attracted to the surface and, hence, tend to be paired with chloride anions or solvated on much shorter times. The results observed in Figure 8 for the charged nanomembranes with *local charges* are intermediate between the two cases described above; for both systems, the time correlation functions are difficult to predict as they depend on a subtle competition between the strong cation/charged surface interaction and self-diffusion of the confined aqueous electrolyte. Nevertheless, it must be noted that, as expected, the decay observed in the time correlation functions for the charged nanomembranes with *local charges* becomes faster as the surface charge increases (i.e., the dynamics of the adsorbed

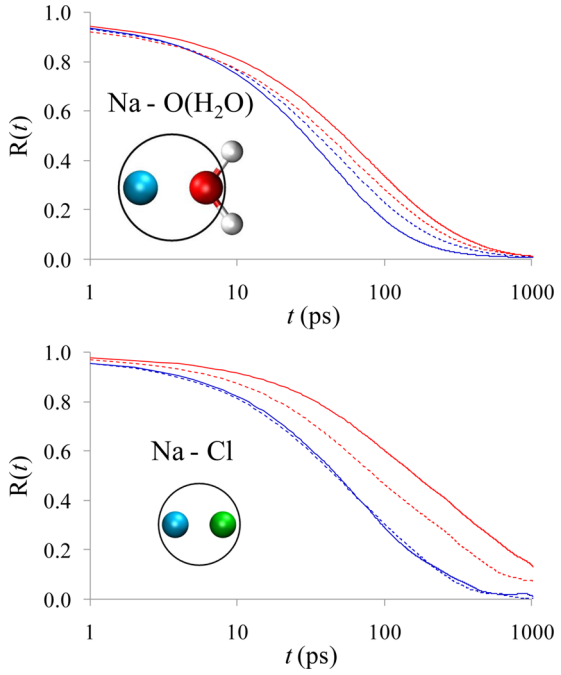

Figure 8. (a) Time correlation function $R(t)$ between the sodium cations Na and oxygen atoms O of the water molecules of an aqueous electrolyte NaCl (1.85 mol/L) confined in a charged nanomembrane with a diameter D = 3 nm carrying either a *diffuse charge* (solid lines) or *local charges* (dashed lines). The blue and red data are for a total electrostatic charge of −0.9 e/nm^2 or −1.8 e/nm^2. (b) Time correlation function $R(t)$ between the sodium cations Na and chloride anions Cl of an aqueous electrolyte NaCl (1.85 mol/L) confined in a charged nanomembrane with a diameter D = 3 nm carrying either a *diffuse charge* (solid lines) or *local charges* (dashed lines). The blue and red data are for a total electrostatic charge of −0.9 e/nm^2 or −1.8 e/nm^2.

sodium counterions becomes slower as they get strongly physisorbed in the charged sites of the nanomembrane so that, in turn, they get paired or solvated on much shorter times). We also note that the time correlation functions between the chloride anions and hydrogen atoms of water confirm the interpretation above (results not shown).

To complete our investigation of the dynamics of the confined aqueous electrolyte, we also determine the residence function of water at the nanomembrane surface

$$P(t) = \frac{1}{N} \sum_{i=1}^{N} \langle \Theta_i(0)\Theta_i(t) \rangle \quad (7)$$

where $\Theta_i(t)$ now equals 1 if the water molecule i is located at time t within the first adsorbed layer and 0 otherwise. N is the total number of water molecules. The latter function differs from that in eq 3 as it provides an estimate of the average time spent by the water molecules in the vicinity of the nanomembrane surface.[51,82,83] Figure 9 shows $P(t)$ for the water molecules of the aqueous electrolyte confined in the different charged nanomembranes. The different sets of results, which follow the same trend as that observed in the time correlation functions in Figure 8, confirm the interpretation above. The shortest residence time (i.e., fastest decay in the residence function) is observed for the weakly charged nanomembrane with a *diffuse charge*. Such a behavior is due to the fast diffusion of the water molecules that tend not to stick to the nanomembrane surface for long times (we recall

dx.doi.org/10.1021/jp4098638 | J. Phys. Chem. C 2014, 118, 5061−5072

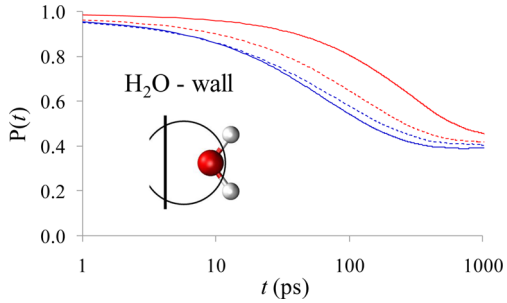

Figure 9. Residence function $P(t)$ of the oxygen atoms O of the water molecules at the nanomembrane surface for an aqueous electrolyte NaCl (1.85 mol/L) confined in a charged nanomembrane with a diameter D = 3 nm carrying either a *diffuse charge* (solid lines) or *local charges* (dashed lines). The blue and red data are for a total electrostatic charge of −0.9 e/nm^2 or −1.8 e/nm^2.

that the water self-diffusion for this charged nanomembrane is even larger than that for the neutral nanomembrane). In contrast, due to the strong interaction with the numerous charges at the nanomembrane surface, the water molecules tend to stick on much longer times when the electrolyte is confined in the highly charged nanomembrane with a *diffuse charge*. Finally, the nanomembranes with *local charges* seem to correspond to intermediate situations where the average residence time of water at the nanomembrane surface depends in a simple fashion on the overall nanomembrane charge; i.e., due to the Coulombic interaction with the *local charges*, the diffusion of water becomes slower as the total charge increases and sticks on longer times to the surface.

4. CONCLUSION

This paper reports a Molecular Dynamics study of an aqueous electrolyte NaCl confined in nanomembranes with a negatively charged surface. Both nanomembranes with a *diffuse charge* and with *local charges* are considered (in both cases, two surface charge densities are considered, −0.9 e/nm^2 and −1.8 e/nm^2). For all nanomembranes, significant layering of water in the vicinity of the nanomembrane surface is observed. On the other hand, beyond the first two adsorbed layers, the water density tends toward the bulk value as water recovers its bulk properties. While the distribution of confined water and chloride anions is nearly insensitive to the charge and type of nanomembrane, the arrangement of the sodium cations within the negatively charged nanomembrane depends on the type and charge of nanomembrane being considered. We compare the water and ion density profiles in the nanomembranes with the predictions of a modified Poisson−Boltzmann equation in which charge image, solvation effects, and dispersion interactions with the surface are taken into account. While including external interactions with the surface atoms (i.e., besides the Coulombic interactions) allows predicting the position of the first ion density peaks, including the local polarization leads to little improvement. We also find that although it constitutes an improvement compared to the conventional Poisson−Boltzmann equation, such a modified Poisson−Boltzmann equation does not capture the structure of the confined electrolyte beyond the first adsorbed layer. It should be emphasized that the nonobservation in the present work of the double electrical layer and the inaccuracy of the modified Poisson−Boltzmann equation to capture all the richness of the structure of the confined electrolyte are probably due to the large ion concentration considered in our systems (1.85 mol/L). The corresponding Debye length is very small ∼10^{-1} nm so that so-called ion specific effects and crowding effects, which are particularly important in such small nanopores, become predominant. In particular, such a large ion concentration leads to steric and size correlations, which cannot be captured by a mean-field approach such as the Poisson−Boltzmann equation.

For all species of the confined electrolyte (Na, Cl, H_2O) and all charged nanomembranes, the Fickian diffusive regime in the direction parallel to the nanomembrane axis is reached in the limit of long times. In contrast, no diffusion perpendicularly to the pore surface is observed due to spatial confinement in the nanomembrane. For all nanomembranes, the self-diffusion coefficient for a given species is smaller than its bulk counterpart and is at most 75% of the bulk value. Our results show that the self-diffusion coefficients of the electrolyte along the pore axis depend in a simple manner on the type and charge of the nanomembrane. Both the self-diffusion coefficients for water and sodium cations decrease with decreasing the overall charge of the nanomembrane, due to the decrease in their Coulombic interaction with the charged surface. In contrast, the self-diffusion coefficient for the chloride anions is nearly independent of the type and charge of the nanomembrane as their properties do not directly depend on the negatively charged surface (the anion/negatively charged surface interaction is screened by the sodium cations located close to the nanomembrane). In contrast to the structural and self-dynamical properties, the residence time, pairing time, and solvation time of the confined electrolyte do not depend in a simple manner on the type and charge of the nanomembrane. The solvation, residence, and pairing times depend on a subtle balance between the average diffusivity and distribution of the confined aqueous electrolyte.

■ ASSOCIATED CONTENT

Ⓢ Supporting Information

Derivation of the modified Poisson−Boltzmann equation for the cylindrical geometry and the density profiles showing the structure of the confined electrolytes. This material is available free of charge via the Internet at http://pubs.acs.org.

■ AUTHOR INFORMATION

Corresponding Author

*E-mail: coasne@mit.edu.

Notes

The authors declare no competing financial interest.

■ ACKNOWLEDGMENTS

We thank the French National Research Agency (ANR) for funding through the research project "SIMONANOMEM" (ANR-07-NANO-055-04). R.H. and B.C. acknowledge financial support from the Région Languedoc-Roussillon (France) through the research grant "Chercheur(se)s d'Avenir 2011". We thank Prof. Lydéric Bocquet for his help with the modified Poisson−Boltzmann equation and stimulating discussions. We also thank Dr. John Palmeri for very helpful discussions.

■ REFERENCES

(1) Bocquet, L.; Charlaix, E. Nanofluidics, from bulk to interfaces. *Chem. Soc. Rev.* **2010**, *39*, 1073.

(2) Hagg, M. B. Membranes in chemical processing. A review of applications and novel developments. *Sep. Purif. Methods* **1998**, *27*, 51.

(3) Shannon, M. A.; Bohn, P. W.; Elimelech, M.; Georgiadis, J. G.; Marinas, B. J.; Mayes, A. M. Science and technology for water purification in the coming decades. *Nature* **2008**, *452*, 301.
(4) Choi, W.; Ulissi, Z. W.; Shimizu, S. F. E.; Bellisario, D. O.; Ellison, M. D.; Strano, M. S. Diameter-dependent ion transport through the interior of isolated single-walled carbon nanotubes. *Nat. Commun.* **2013**, *4*, 2397.
(5) Lefebvre, X.; Palmeri, J.; David, P. Nanofiltration theory: An analytic approach for single salts. *J. Phys. Chem. B* **2004**, *108*, 16811.
(6) Chmiel, H. Lefebvre, X. Mavrov, V. Noronha, M.; Palmeri, J. J. Computer Simulation of Nanofiltration, Membranes and Processes. In *Handbook of Theoretical and Computational Nanotechnology*; Rieth, M.; Schommers, W., Eds.; American Scientific Publishers: Los Angeles, CA, 2006; Vol. 5, pp 93−214.
(7) http://news.bbc.co.uk/2/hi/europe/8161889.stm (accessed July 21, 2009).
(8) Cazade, P.-A.; Dweik, J.; Coasne, B.; Henn, F.; Palmeri, J. Molecular simulation of ion-specific effects in confined electrolyte solutions using polarizable forcefields. *J. Phys. Chem. C* **2010**, *114*, 12245.
(9) Chandler, D. Interfaces and the driving force of hydrophobic assembly. *Nature* **2005**, *437*, 640.
(10) Jungwirth, P.; Tobias, D. J. Specific ion effects at the air/water interface. *Chem. Rev.* **2006**, *106*, 1259.
(11) Sparreboom, W.; van den Berg, A.; Eijkel, J. C. T. *Nat. Nanotechnol.* **2009**, *4*, 713.
(12) Christenson, H. K.; Claesson, P. M. Direct measurements of the force between hydrophobic surfaces in water. *Adv. Colloid Interface Sci.* **2001**, *91*, 391.
(13) Meyer, E. E.; Rosenberg, K. J.; Israelachvili, J. Recent progress in understanding hydrophobic interactions. *Proc. Nat. Acad. Sci. U.S.A.* **2006**, *103*, 15739.
(14) Huang, D. M.; Cottin-Bizonne, C.; Ybert, C.; Bocquet, L. Massive amplification of surface-induced transport at superhydrophobic surfaces. *Phys. Rev. Lett.* **2008**, *101*, 064503.
(15) Xue, J. M.; Zou, X. Q.; Xie, Y. B.; Wang, Y. G. Molecular dynamics simulations on the ionic current through charged nanopores. *J. Phys. D: Appl. Phys.* **2009**, *42*, 105308.
(16) Suk, M. E.; Aluru, N. R. Effect of induced electric field on single-file reverse osmosis. *Phys. Chem. Chem. Phys.* **2009**, *11*, 8614.
(17) Huang, D. M.; Cottin-Bizonne, C.; Ybert, C.; Bocquet, L. Aqueous electrolytes near hydrophobic surfaces: Dynamic effects of ion specificity and hydrodynamic slip. *Langmuir* **2008**, *24*, 1442.
(18) Caldwell, J. W.; Dang, L. X.; Kollman, P. A. Implementation of nonadditive intermolecular potentials by use of Molecular Dynamics—Development of a water water potential and water ion cluster interactions. *J. Am. Chem. Soc.* **1990**, *112*, 9145.
(19) Dang, L. X.; Rice, J. E.; Caldwell, J. W.; Kollman, P. A. Ion solvation in polarizable water—Molecular Dynamics simulations. *J. Am. Chem. Soc.* **1991**, *113*, 2481.
(20) Perera, L.; Berkowitz, M. L. Many-body effects in molecular dynamics simulations of Na+(H_2O)n and Cl-(H_2O)n clusters. *J. Chem. Phys.* **1991**, *95*, 7556.
(21) Caldwell, J. W.; Kollman, P. A. Cation-PI interactions—Nonadditive effects are critical in their accurate representation. *J. Am. Chem. Soc.* **1995**, *117*, 4177.
(22) Shelley, J. C.; Sprik, M.; Klein, M. L. Molecular dynamics simulation of an aqueous sodium octanoate micelle using polarizable surfactant molecules. *Langmuir* **1993**, *9*, 916.
(23) Marrone, T. J.; Hartsough, D. S.; Merz, K. M. J. Determination of atomic charges including solvation and conformational effects. *J. Phys. Chem.* **1994**, *98*, 1341.
(24) Gregory, J. K.; Clary, D. C.; Liu, K.; Brown, M. G.; Saykally, R. J. The water dipole moment in in water clusters. *Science* **1997**, *275*, 814.
(25) Dang, L. X.; Chang, T. M. Molecular dynamics study of water clusters, liquid, and liquid−vapor interface of water with many-body potentials. *J. Chem. Phys.* **1997**, *106*, 8149.
(26) Dang, L. X. Importance of polarization effects in modeling the hydrogen bond in water using classical molecular dynamics techniques. *J. Phys. Chem.* **1998**, *102*, 620.
(27) Herce, D. H.; Perera, L.; Darden, T. A.; Sagui, C. Surface solvation for an ion in a water cluster. *J. Chem. Phys.* **2005**, *122*, 24513.
(28) Chang, T. M.; Dang, L. X. Recent advances in molecular simulations of ion solvation at liquid interfaces. *Chem. Rev.* **2005**, *106*, 1305.
(29) Horinek, D.; Netz, R. R. Specific ion adsorption at hydrophobic solid surfaces. *Phys. Rev. Lett.* **2007**, *99*, 226104.
(30) Dweik, J.; Coasne, B.; Palmeri, J.; Jouanna, P.; Gouze, P. Inner and Subsurface Distribution of Water and Ions in Weakly and Highly Hydrophilic Uncharged Nanoporous Materials: A Molecular Dynamics Study of a Confined NaI Electrolyte Solution. *J. Phys. Chem. C* **2012**, *116*, 726.
(31) Whitby, M.; Quirke, N. Fluid flow in carbon nanotubes and nanopipes. *Nat. Nanotechnol.* **2007**, *2*, 87.
(32) Falk, K.; Sedlmeier, F.; Joly, L.; Netz, R.; Bocquet, L. Molecular Origin of Fast Water Transport in Carbon Nanotube Membranes: Superlubricity versus Curvature Dependent Friction. *Nano Lett.* **2010**, *10*, 4067.
(33) Horvath, L.; Beu, T.; Manghi, M.; Palmeri, J. The vapor-liquid interface potential of (multi)polar fluids and its influence on ion solvation. *J. Chem. Phys.* **2013**, *138*, 154702.
(34) Caldwell, J. W.; Kollman, P. A. Structure and properties of neat liquids using non additive molecular dynamics—water, methanol, and n-methylacetamide. *J. Phys. Chem.* **1995**, *99*, 6208.
(35) Dang, L. X. Development of nonadditive intermolecular potentials using molecular dynamics: Solvation of Li+ and F- ions in polarizable water. *J. Chem. Phys.* **1992**, *96*, 6970.
(36) Xantheas, S. S.; Dang, L. X. Critical study of fluoride water interactions. *J. Phys. Chem.* **1996**, *100*, 3989.
(37) Chang, T.; Dang, L. X. Molecular dynamics simulations of CCl_4-H_2O liquid-liquid interface with polarizable potential models. *J. Chem. Phys.* **1996**, *104*, 6772.
(38) Dang, L. X. Computational study of ion binding to the liquid interface of water. *J. Phys. Chem. B* **2002**, *106*, 10388.
(39) Rowlinson, J. *Liquids and Liquid Mixtures*; Springer: New York, 1995.
(40) Ren, P.; Ponder, J. W. Consistent treatment of inter- and intramolecular polarization in molecular mechanics calculations. *J. Comput. Chem.* **2002**, *23*, 1497.
(41) Bonnaud, P. A.; Coasne, B.; Pellenq, R. M. J. Molecular simulation of water confined in nanoporous silica. *J. Phys.: Condens. Matter* **2010**, *22*, 284110.
(42) Allen, M. P.; Tildesley, D. J. *Computer Simulation of Liquids*; Oxford University Press: New York, 1989.
(43) Frenkel, D.; Smit, B. *Understanding Molecular Simulation: From Algorithms to Applications*, 2nd ed.; Academic Press: New York, 2001.
(44) Case, D. A.; Darden, T. A.; Cheatham, T. E., III; Simmerling, C. L.; Wang, J.; Duke, R. E.; Luo, R.; Merz, K. M.; Pearlman, D. A.; Crowley, M.; Walker, R. C.; Zhang, W.; Wang, B.; Hayik, S.; Roitberg, A.; Seabra, G.; Wong, K. F.; Paesani, F.; Wu, X.; Brozell, S.; Tsui, V.; Gohlke, H.; Yang, L.; Tan, C.; Mongan, J.; Hornak, V.; Cui, G.; Beroza, P.; Mathews, D. H.; Schafmeister, C.; Ross, W. S.; Kollman, P. A. *AMBER 9*; University of California: San Francisco, 2006.
(45) Alexiadis, A.; Kassinos, S. Molecular simulation of water in carbon nanotubes. *Chem. Rev.* **2008**, *108*, 5014.
(46) Hummer, G.; Rasaiah, J. C.; Noworyta, J. P. Water conduction through the hydrophobic channel of a carbon nanotube. *Nature* **2001**, *414*, 188.
(47) Koga, K.; Gao, G. T.; Tanaka, H.; Zeng, X. C. Formation of ordered ice nanotubes inside carbon nanotubes. *Nature* **2001**, *412*, 802−805.
(48) Kolesnikov, A. I.; Zanotti, J.; Loong, C.; Thiyagarajan, P.; Moravsky, A. P.; Loutfy, R. O.; Burnham, C. J. Anomalously soft dynamics of water in a nanotube: a revelation of nanoscale confinement. *Phys. Rev. Lett.* **2004**, *93*, 035503.

(49) Argyris, D.; Cole, D. R.; Striolo, A. Hydration structure on crystalline silica substrates. *Langmuir* **2009**, *25*, 8025.
(50) Giovambattista, N.; Rossky, P. J.; Debenedetti, P. G. Phase behavior and structure of water confined between nanoscale hydrophobic and hydrophilic plates. *Phys. Rev. E* **2006**, *73*, 041604.
(51) Gallo, P.; Rapinesi, M.; Rovere, M. Confined water in the low hydration regime. *J. Chem. Phys.* **2002**, *117*, 369.
(52) Siboulet, B.; Coasne, B.; Dufreche, J. F.; Turq, P. Hydrophobic transition in porous amorphous silica. *Mol. Phys.* **2011**, *115*, 7881.
(53) Alabarse, F. G.; Haines, J.; Cambon, O.; Levelut, C.; Bourgogne, D.; Haidoux, A.; Granier, D.; Coasne, B. Freezing of Water Confined at the Nanoscale. *Phys. Rev. Lett.* **2012**, *109*, 035701.
(54) Markesteijn, A. P.; Hartkamp, R.; Luding, S.; Westerweel, J. A comparison of the value of viscosity for several water models using Poiseuille flow in a nano-channel. *J. Chem. Phys.* **2012**, *136*, 134104.
(55) Bazant, M. Z.; Storey, B. D.; Kornyshev, A. A. Double Layer in Ionic Liquids: Overscreening versus Crowding. *Phys. Rev. Lett.* **2011**, *106*, 046102.
(56) Storey, B. D.; Bazant, M. Z. Effects of electrostatic correlations on electrokinetic phenomena. *Phys. Rev. E* **2012**, *86*, 056303.
(57) Gillespie, D. Free-Energy Density Functional of Ions at a Dielectric Interface. *J. Phys. Chem. Lett.* **2011**, *2*, 1178.
(58) Joly, L.; Ybert, C.; Trizac, E.; Bocquet, L. Hydrodynamics within the Electric Double Layer on Slipping Surfaces. *Phys. Rev. Lett.* **2004**, *93*, 257805.
(59) Kirby, B. *Micro- and Nanoscale Fluid Mechanics*, 1st ed.; Cambridge University Press: New York, 2010; Vol. *32*.
(60) Forsman, J. A simple correlation-corrected Poisson-Boltzmann theory. *J. Phys. Chem. B* **2004**, *108*, 9236.
(61) Antypov, D.; Barbosa, M. C.; Holm, C. Incorporation of excluded-volume correlations into Poisson-Boltzmann theory. *Phys. Rev. E* **2005**, *71*, 061106.
(62) Fraenkel, D. Simplified electrostatic model for the thermodynamic excess potentials of binary strong electrolyte solutions with size-dissimilar ions. *Mol. Phys.* **2010**, *108*, 1435.
(63) Eisenberg, B.; Hyon, Y.; Liu, C. Energy variational analysis of ions in water and channels: Field theory for primitive models of complex ionic fluids. *J. Chem. Phys.* **2010**, *133*, 104104.
(64) Borukhov, I.; Andelman, D.; Orland, H. Steric effects in electrolytes: A modified Poisson-Boltzmann equation. *Phys. Rev. Lett.* **1997**, *79*, 435.
(65) Ben-Yaakov, D.; Andelman, D.; Podgornik, D.; Harries, D.. Ion-specific hydration effects: Extending the Poisson-Boltzmann theory. *Curr. Opin. Colloid Interface Sci.* **2011**, *16*, 542.
(66) Lopez-Garcia, J. J.; Horno, J.; Grosse, C. Poisson-Boltzmann description of the electrical double layer including ion size effects. *Langmuir* **2011**, *27*, 13970.
(67) Wei, G.; Zheng, Q.; Chen, Z.; Xia, K. Variational multiscale models for charge transport. *SIAM Rev.* **2012**, *54*, 699.
(68) Fawcett, W. R. *Liquids, Solutions, and Interfaces: From Classical Macroscopic Descriptions to Modern Microscopic Details*; Oxford University Press: New York, 2004.
(69) Bikerman, J. J. *Philos. Mag.* **1942**, *33*, 384.
(70) Dubbeldam, D.; Snurr, R. Q. Recent developments in the molecular modeling of diffusion in nanoporous materials. *Mol. Simul.* **2007**, *33*, 305.
(71) Hahn, K.; Karger, J. Deviations from the normal time regime of single-file diffusion. *J. Phys. Chem. B* **1998**, *102*, 5766.
(72) Liu, Y.; Shen, J.; Gubbins, K. E.; Moore, J. D.; Wu, T.; Wang, Q. Diffusion dynamics of water controlled by topology of potential energy surface inside carbon nanotubes. *Phys. Rev. B* **2008**, *77*, 125438.
(73) Moore, J. D.; Palmer, J. C.; Liu, Y.; Roussel, T. J.; Brennan, J. K.; Gubbins, K. E. Adsorption and diffusion of argon confined in ordered and disordered microporous carbons. *Appl. Surf. Sci.* **2010**, *256*, 5131.
(74) Schoen, M.; Cushman, J. H.; Diestler, D. J.; Rhykerd, C. L. Fluids in micropores. II. Self-diffusion in a simple classical fluid in a slit pore. *J. Chem. Phys.* **1988**, *88*, 1394.
(75) Diestler, D. J.; Schoen, M.; Hertzner, A. W.; Cushman, J. H. Fluids in micropores. III. Self-diffusion in a slit-pore with rough hard walls. *J. Chem. Phys.* **1991**, *95*, 5432.
(76) Krishnan, S. H.; Ayappa, K. G. Modeling velocity autocorrelation functions of confined fluids: A memory function approach. *J. Chem. Phys.* **2003**, *118*, 690.
(77) Coasne, B.; Jain, S. K.; Gubbins, K. E. Adsorption, structure and dynamics of fluids in ordered and disordered models of porous carbons. *Mol. Phys.* **2006**, *104*, 3491.
(78) Coasne, B.; Alba-Simionesco, C.; Audonnet, F.; Dosseh, G.; Gubbins, K. E. Adsorption, structure and dynamics of benzene in ordered and disordered porous carbons. *Phys. Chem. Chem. Phys.* **2011**, *13*, 3748.
(79) Hawlicka, E.; Swiatla-Wojcik, D. Dynamic properties of the NaCl/methanol/water systems. MD simulation studies. *Phys. Chem. Chem. Phys.* **2000**, *2*, 3175−3180.
(80) Levitz, P. Random flights in confining interfacial systems. *J. Phys.: Condens. Matter* **2005**, *17*, S4059.
(81) Levitz, P.; Bonnaud, P. A.; Cazade, P. A.; Pellenq, R. J. M.; Coasne, B. Molecular intermittent dynamics of interfacial water: probing adsorption and bulk confinement. *Soft Matter* **2013**, *9*, 8654.
(82) Argyris, D.; Cole, D. R.; Striolo, A. Dynamic behavior of interfacial water at the silica surface. *J. Phys. Chem. C* **2009**, *113*, 19591.
(83) Coasne, B.; Viau, L.; Vioux, A. Loading-controlled stiffening in nanoconfined ionic liquids. *J. Phys. Chem. Lett.* **2011**, *2*, 1150.